Journal of Alloys and Compounds 872 (2021) 159636

Contents lists available at ScienceDirect

Journal of Alloys and Compounds

journal homepage: www.elsevier.com/locate/jalcom

Martensite formation in titanium alloys: Crystallographic and compositional effects

Madeleine Bignon[a,b], Emmanuel Bertrand[a], Pedro E.J. Rivera-Díaz-del-Castillo[b,*], Franck Tancret[a]

[a] Institut des Matériaux Jean Rouxel (IMN), Université de Nantes, CNRS, Polytech Nantes, Rue Christian Pauc, 44306 Nantes Cedex 3, France
[b] Department of Engineering, Lancaster University, Lancaster LA1 4YK, UK

ARTICLE INFO

Article history:
Received 8 February 2021
Received in revised form 8 March 2021
Accepted 20 March 2021
Available online 26 March 2021

Keywords:
Titanium
Martensite
Phenomenological theory of martensitic transformation
Superelasticity
Transformation induced plasticity

ABSTRACT

An explanation is proposed to martensite inhibition beyond characteristic concentration thresholds in titanium binary alloys. The method combines the phenomenological theory of martensite crystallography (PTMC) and thermodynamic calculations (TCs) to describe the conditions under which martensite formation is favourable. It is shown that martensite can be crystallographically prevented while being thermodynamically favourable. The PTMC is implemented by taking into account the influence of composition. After a comprehensive comparison to experiments, two twinning systems and two glide systems are inferred to be able to produce the lattice invariant shear. The critical concentrations above which martensite cannot form are computed and compared to experimental results on binary and ternary systems, showing good agreement. The proposed method may be used as a guide to design titanium alloys for controlled martensitic behaviour.

1. Introduction

Martensitic transformation is responsible for some of the most interesting mechanical properties of titanium alloys. The formation of martensite can induce shape memory and superelastic effects [1–3], which both have application in biomedical industry, or can improve ductility and work-hardening via transformation induced plasticity (TRIP) [4–7]. In the past few years, there has been an increasing interest in designing titanium alloys displaying martensitic transformation. In order to improve design methods, it is useful to understand the composition dependency of martensite formation. The present work aims at showing how the composition-dependent geometric accommodation of martensite can control the occurrence of the transformation.

Binary titanium alloys are known to undergo martensitic transformation under a variety of conditions [8] (Fig. 1). In pure titanium, martensite forms upon quenching from the high temperature body centered cubic (bcc) β-phase field [8]. The addition of elements known as β-stabilizers (e.g. Fe, Cr, Mo, V, Nb, Ta and W) contributes to stabilize the β-phase at the expense of martensite. Martensite displays hexagonal close-packed (hcp) α' or orthorhombic α" structure, depending on composition [8]. For the purpose of the mathematical modelling presented here, the hcp structure can be described as an orthorhombic structure where $b = \sqrt{3}a$. Therefore, martensite will be here referred to in a more general way as α^m, as in [9]. Dilute alloys usually display martensite upon quenching; when increasing the concentration of β-stabilizers above a certain threshold (labelled β_c on Fig. 1), martensite only forms upon deformation until, with further increasing concentration, no martensite forms anymore, neither upon quenching nor deformation [10]. For each alloying element, the minimal concentration necessary to prevent martensite formation is called β_d.[1] The values of β_d for different binary systems are reported in Table 1. The present work focuses on the reason why martensite stops forming beyond a certain elemental concentration.

The chemical driving force for martensite transformation (Δg_{ch}) is generally thought to be the key factor controlling martensite formation. $\Delta g_{ch} = g_\beta - g_{\alpha^m}$, where g_β and g_{α^m} are respectively the Gibbs free energies of the parent β phase and of the martensite product phase. It is commonly reported that the inhibition of martensite for an elemental concentration above β_d is due to Δg_{ch} being too low to compensate for the energy terms opposing the transformation, i.e. interfacial energy and elastic strain energy. To test this hypothesis, Δg_{ch} was computed at room temperature as a function of composition

* Corresponding author.
E-mail address: p.rivera1@lancaster.ac.uk (P.E.J. Rivera-Díaz-del-Castillo).

[1] Some systems, such as Ti-Fe or Ti-Cr have not been reported to display martensite upon deformation, for those, $\beta_c = \beta_d$.

https://doi.org/10.1016/j.jallcom.2021.159636
0925-8388/

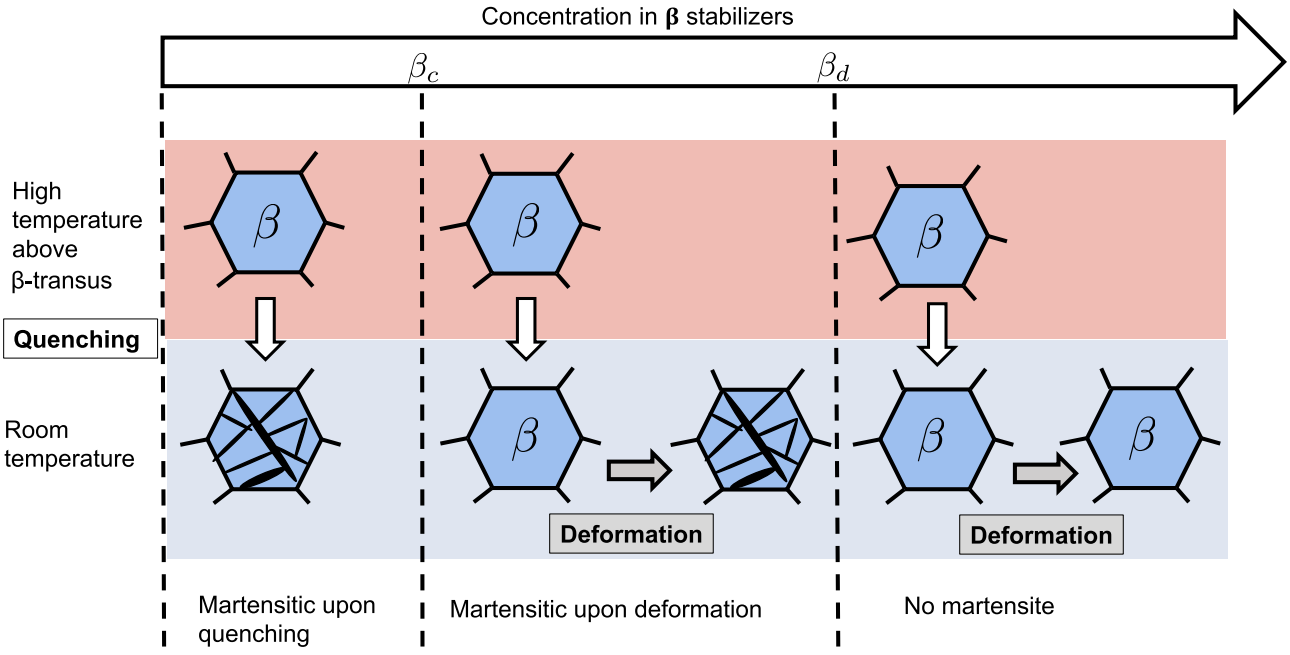

Fig. 1. Transitions exhibited by binary Ti systems.

Table 1
Critical concentration β_d beyond which martensite has never been reported in binary alloys, neither upon quenching nor deformation.

Binary system	β_d wt%	β_d at%	References
Ti-Fe	3.5–4.6	3–4	[11]
Ti-V	16–20	15.2–19	[12–14]
Ti-Mo	14–16	7.5–8.7	[13–16]
Ti-Cr	5.6–7.4	5.2–6.85	[17,18]
Ti-Zr	100	100	[19]
Ti-Ta	72–76	40–45	[20]
Ti-Nb	40–42.5	25.7–27.8	[21]
Ti-W	29.9–32.2	10–11	[22]
Ti-Os	7.5–10.9	2–3	[22]

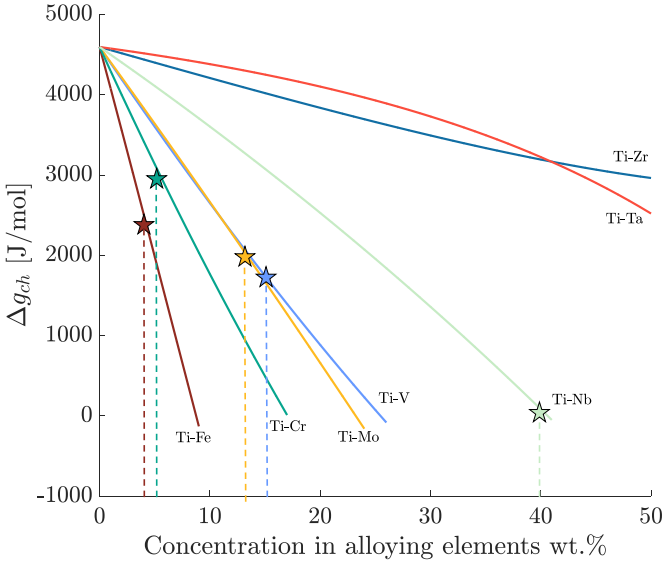

Fig. 2. Computation of the driving force for martensite formation at room temperature. The stars represent, for each system, the critical concentration above which martensite has not been experimentally reported upon quenching or deformation. The experimental observations are collected from [11] for Ti-Fe, [17,32,33] for Ti-Cr, [34,35,14,36,13] for Ti-V, [34,15,37,14,16] for Ti-Mo, [17,28] for Ti-Ta and [38,21,39,40] for Ti-Nb.

in different binary systems, as shown in Fig. 2. The calculations were performed with CALculation of PHAse Diagrams (Calphad) method, using the "TCTI1" thermodynamic titanium database of Thermo-Calc® software. The free energy of the martensite is assumed to equal that of the hcp phase; this approximation has been used and discussed before [23–25]. The critical concentrations β_d of the different elements are also displayed in Fig. 2. It is apparent from the figure that the values of β_d correspond to highly scattered values of Δg_{ch} which are not close to zero. The situation is more pronounced for systems such as Ti-Fe and Ti-Cr, where martensite does not form, even under stress, at values of Δg_{ch} largely exceeding that of the elastic energy opposing the transformation (~100 J/mol for thermoelastic martensite [26]). It follows that thermodynamic considerations alone cannot explain the formation of martensite and the stabilization of β-phase.

In the present work, the phenomenological theory of martensite crystallography (PTMC) is adopted to explain the absence of martensite as being due to the lack of plausible shear systems to undergo the transformation via an invariant plane strain (IPS). The PTMC is a well-established tool that allows to explain and interpret the crystallographic features of the observed martensite. For example, the composition dependency of the coordinates of the habit planes of martensite plates have been investigated in various binary and ternary titanium alloys [27–30,31]. However, to the best of our knowledge, no previous attempt has been made to extend the calculations to compositions where martensite is not observed. By showing that for these compositions it is impossible to form martensite through an IPS, the present work proposes an interpretation to martensite inhibition in titanium alloys.

2. Main principles of the PTMC and hypothesis of this work

2.1. Invariant plane strain problem

The PTMC, independently developed by Wechsler et al. [41] and Bowles and Mackenzie [42–45], and summarised for instance in [46,47], solved an apparent contradiction between experimental observations and crystallography. When a martensite plate forms in a metal on the surface of which straight lines have been drawn before transformation, the initially flat surface is tilted, the broken line elements remain straight, and the interface between the

martensite plates and the matrix remains continuous. This can only be possible if the interface plane, called habit plane, remains undistorted and unrotated during the transformation. Such a transformation is called an invariant plane strain (IPS) [42]. However, in most martensitic transformations, the crystallography of the parent and product lattices are such that one lattice cannot be transformed into the other by an IPS. There was therefore an inconsistency between the lattice transformation and the macroscopic observations. The authors of the PTMC [42,43] solved this puzzle by describing the transformation in terms of a total lattice deformation that homogeneously transforms the parent lattice into a plate of product lattice, followed by a so-called lattice invariant shear (LIS). The LIS takes place inhomogeneously, meaning that the plate is not sheared as a whole but in segments, maintaining the crystallographic structure after the total lattice deformation, while allowing the average interface plane (macroscopic habit plane) to be invariant. The LIS can be produced either by twinning of the product lattice or by dislocation glide.

2.2. Inputs and outputs of the PTMC

The PTMC allows to solve the IPS problem, or in other words to determine along which habit planes martensite can form with a macroscopically invariant plane strain. If a solution to this problem exists, the outputs of the calculation procedure are the coordinates of the habit plane, the volumetric fraction f_{tw} of a martensite plate being internally twinned by the LIS or the number of interface dislocations, as well as the total average strain. In order to calculate these features, three inputs are necessary. The first one is the lattice correspondence between martensite and parent phase; this is well established in Ti alloys and given in Appendix A. Second, the eigenvalues of the lattice transformation, labelled η_1, η_2 and η_3 are required [45]. They are determined by the lattice parameters of both the parent and the product phases via:

$$\eta_1 = \frac{a}{a_\beta}$$
$$\eta_2 = \frac{b}{\sqrt{2}\cdot a_\beta}$$
$$\eta_3 = \frac{c}{\sqrt{2}\cdot a_\beta} \quad (1)$$

where a, b and c are the lattice parameters of the martensite[2] and a_β is the lattice parameter of the parent bcc phase. The lattice parameters depend on composition, as described in Section 3. Third, the plane and direction in which the LIS takes place need to be determined [45]. The coordinates of the planes and directions can be defined in the initial parent lattice, in the product lattice or in the eigenbase. The correspondence between the coordinates are provided in Appendix A. Hereon, **h** and **u** are unit vectors parallel to the initial positions of the normal to the shear plane and the shear direction of the LIS, respectively. The coordinates of **h** in the eigenbase will be denoted (h_1, h_2, h_3) and those of **u** will be denoted $[u_1; u_2; u_3]$, where comas refer to row vectors and semicolons to column vectors. It is not universally accepted which LIS systems are involved in Ti alloys; different possibilities have been considered in the literature [45,48,28]. The selection of potential LIS systems is addressed in Section 3.1. It should be noted that when the LIS mechanism is twinning, then either **h** or **u** depend on the composition, given that the twinning elements depend on the lattice parameters.

[2] a and b are independent in the case of an orthorhombic martensite whereas $b = a\cdot\sqrt{3}$ if the martensite has an hcp structure

2.3. Conditions for the existence of a solution to the IPS problem

The existence of a solution to the IPS problem depends on the eigenvalues of the transformation and on the LIS system. Crocker and Bilby [49] pointed out that two necessary conditions must be simultaneously fulfilled for the IPS problem to have a solution, one concerning the plane of the LIS,

$$h_1^2\cdot(1-\eta_2^2)\cdot(1-\eta_3^2) + h_2^2\cdot(1-\eta_3^2)\cdot(1-\eta_1^2) + h_3^2\cdot(1-\eta_1^2)\cdot(1-\eta_2^2) \le 0 \quad (2)$$

and the other its direction

$$u_1^2\cdot\eta_1^2\cdot(1-\eta_2^2)\cdot(1-\eta_3^2) + u_2^2\cdot\eta_2^2\cdot(1-\eta_3^2)\cdot(1-\eta_1^2) + u_3^2\cdot\eta_3^2\cdot(1-\eta_1^2)\cdot(1-\eta_2^2) \le 0 \quad (3)$$

Assuming that the LIS system (**h** and **u**) is known (section 3.1), a solution to the IPS problem exists as long as Inequations (2) and (3) are met. These conditions are necessary but not sufficient for martensite formation to be possible. Once it is verified that the IPS problem has a solution satisfying (2) and (3), the complete PTMC calculation has to be performed. Indeed, the mathematical solution of the problem may, for instance, lead to a calculated fraction of internally twinned martensite f_{tw} that either exceeds unity or is negative, which is physically impossible. In such case, the solution should be discarded.

2.4. Hypothesis

As discussed above, critical compositions β_d exist beyond which martensite does not form although it appears to be thermodynamically more stable than the β phase (Figs. 1 and 2). On the other hand, when martensite forms, experiments show that the transformation always takes place via an IPS. The hypothesis made here is that the experimental compositional thresholds correspond to the limits of existence of solution to the IPS problem. In other words, the inhibition of martensite would be the consequence of "crystallographic incompatibility", meaning that the parent phase cannot be transformed into martensite via an IPS.

To demonstrate this, we first express the eigenvalues as a function of composition. Second, a list of potential LIS systems is established based on theoretical considerations regarding lattice correspondences and interface mobility along with experimental observations. Once the list of potential LIS systems is established, it is possible, for a given composition to predict whether martensite can form adopting any such LIS system, following the procedure illustrated in Fig. 3. If none of the potential LIS systems allows the transformation, then it can be concluded that martensite formation is inhibited for such composition. If at least one LIS system allows the transformation to take place, the transformation is crystallographically possible. It can then be verified, by computing the chemical driving force and the elastic strain energy as described in Section 5, whether the energy balance favours the transformation.

3. Composition dependency of eigenvalues

The eigenvalues are functions of the lattice parameters (Eq. (1)). In order to derive an expression of the lattice parameters as a function of composition, Vegard's law is adopted, the linear variation of the lattice parameters with the concentration in alloying elements is expressed as:

$$a = a_0 + x_i\Delta a^i$$
$$b = b_0 + x_i\Delta b^i$$
$$c = c_0 + x_i\Delta c^i$$
$$a_\beta = a_{\beta_0} + x_i\Delta a_\beta^i \quad (4)$$

where a_0, b_0 and c_0 are the lattice parameters of martensite in pure Ti, and a_{β_0} is that of the β-phase. Δa^i is the change in lattice

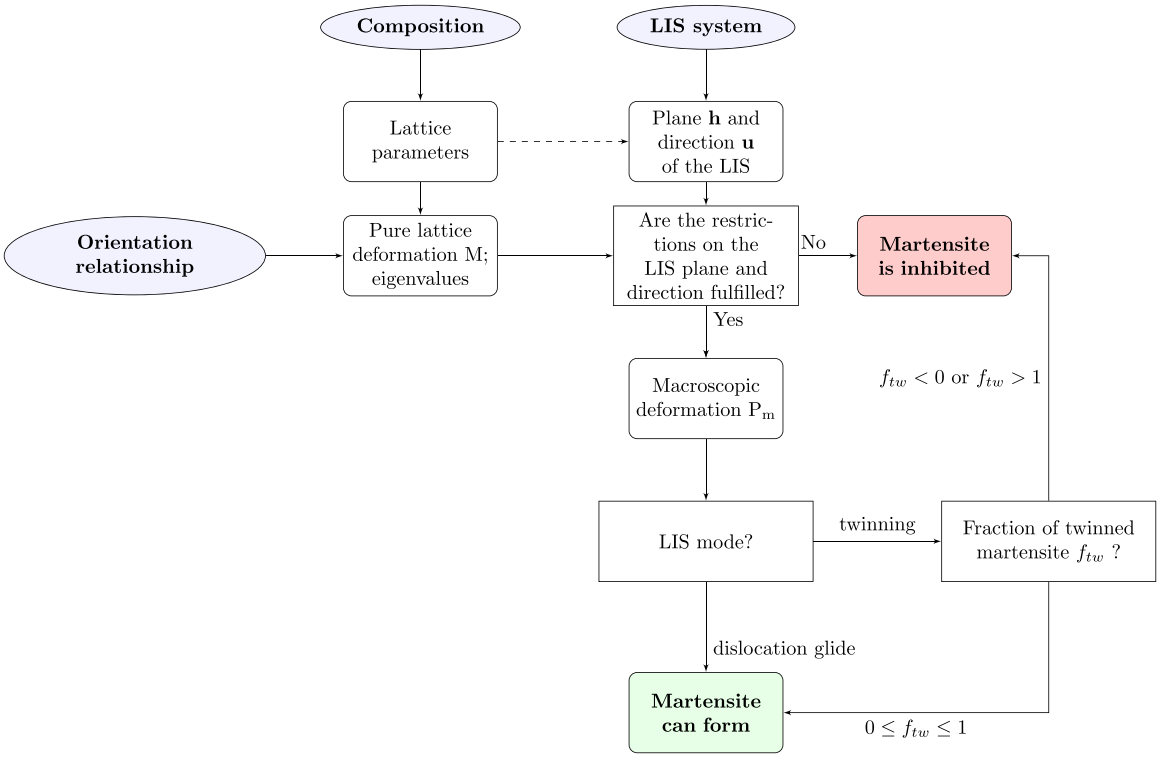

Fig. 3. Procedure to determine whether martensite is inhibited. The PTMC elements are calculated following the method described in [42,43,45]. The dashed arrow only applies if the LIS is accomplished by twinning since in that case, either the shear direction or shear plane depends on the lattice parameters.

Table 2
Lattice parameters for 0% solute element additions [nm].

	a	b	c	References
β	0.3283			[51]
α'	0.2959	$\sqrt{3}a$	0.468	[50]
α"*	0.288	0.5264	0.4734	[50]

* extrapolated from concentrated alloys.

Table 3
Evolution of the lattice parameters upon addition of alloying elements [10^{-3} nm/at%].

	$\Delta a_{\alpha''}$	$\Delta b_{\alpha''}$	$\Delta c_{\alpha''}$	$\Delta a_{\alpha'}$	$\Delta c_{\alpha'}$	Δa_{β}
Fe [11,51]	–	–	–	0	-1.5	-0.54
V [22,54]	+0.62	-1.84	-0.8748	-0.164	-0.297	-0.257
Mo [22,50]	+2.29	-3.16	-1.48	0	+0.2831	-0.1259
Cr [51,55]	–	–	–	-0.26	-1.33	-0.39
Zr [53,56]	+0.9	-0.28	+0.3	+0.22	+0.5	+0.31
Ta [52,57]	+0.9	-1.3856	0	0	+0.5	+0.02
Nb [38]	+1.364	-1.546	-0.238	0	+0.5	+0.013
W [22]	+2.43	-2.46	-0.57	-1.3	-0.4	-0.15
Os [17,22]	+6.3	-8.82	+1.2	–	–	-0.55

parameter of a due to an increase in 1 at% of element i, and x_i is the atomic percent of element i. The values of the lattice parameters in pure titanium for α' are extracted from [50]. Orthorhombic martensite does not form in pure titanium, but the extrapolation of measurements made from concentrated alloys (e.g. Ti-Mo, Ti-Ta, Ti-Nb in [50]) as a function of composition shows that the calculation of the lattice parameters at 0% of solute element leads to the same value for the parameters of α". The adopted lattice parameters of the three crystallographic structures in pure titanium are gathered in Table 2.

Measurements in the literature are scarce and scattered but linear relationships between atomic concentration and lattice parameters are usually found [24,52,53]. It can also be noted that the variation of the lattice parameters is continuous with respect to composition, and that at the compositions where the transition α'/α" takes place, the two crystallographic structures exhibit the same lattice parameters [22,24]. Since the purpose of this work is to describe trends on the martensitic transformation when increasing the concentration in alloying elements, it was chosen to extract such trends from articles where the lattice parameters were consistently measured for different alloys of the same binary or ternary system, in order to reduce bias in the measurements. The used values are gathered in Table 3. Potential consequences on the model will be discussed later.

3.1. Selection of LIS systems

To assess whether the suppression of martensite can be explained by the absence of any solution to the IPS problem, it is necessary to establish a comprehensive list of potential LIS systems. According to the PTMC, the lattice invariant shear can take place by twinning or by dislocation glide. Several studies exploiting the PTMC only focus on twinning as LIS mode [45,58,27]. On the other hand, other authors have reached the conclusion that the LIS should occur by dislocation glide [48]. Given that experiments show both twinned and untwinned martensite [28], both modes are considered here.

3.1.1. Selection of the potential twinning systems

According to the PTMC, in order for a twinning system to be a possible LIS system, the two twins in the product lattice must correspond to two crystallographically equivalent lattices in the parent phase [43]. This condition of equivalent correspondences uniquely determines the four twinning elements if either the twinning direction or the twinning plane is known. It also implies that i) if the twinning plane is rational (twinning of type I), then it has to be generated from a mirror plane in the parent lattice [43] ii) if the

Table 4
Possible twinning systems expressed in the orthorhombic or hcp lattice.

System		Twinning systems in the orthorhombic or hcp lattice
A	Plane	$(1\bar{1}\bar{1})_O$ - $(1\bar{1}0\bar{1})_H$
	Direction	$[4\eta_2^2\eta_3^2 - 2\eta_2^2\eta_1^2 - 2\eta_3^2\eta_1^2, 2\eta_2^2\eta_3^2 + \eta_2^2\eta_1^2 - 3\eta_3^2\eta_1^2, 2\eta_2^2\eta_3^2 - 3\eta_2^2\eta_1^2 + \eta_3^2\eta_1^2]_O$
B	Plane	$(0\bar{1}1)_O$ - $(0\bar{1}12)_H$
	Direction	$[011]_O$ - $[01\bar{1}1]_H$
Type II	Plane	$(\eta_2^2 + \eta_3^2 - 2\eta_1^2, 3\eta_2^2 - \eta_3^2 - 2\eta_1^2, -\eta_2^2 + 3\eta_3^2 - 2\eta_1^2)_O$
	Direction	$[2\bar{1}\bar{1}]_O[4\bar{5}1\bar{3}]_H$

twinning direction is rational (type II), then it has to be generated from a two-fold axis in the parent lattice [58]. Bowles and Mackenzie showed that if the twinning system is assumed to be of type I, only two possible twinning systems meet the condition of equivalent correspondences [43]. These systems are labelled A and B and are reported in Table 4. As far as we are aware the list of all possible type II twinning systems meeting the condition of equivalent correspondences has not been reported in the literature, so we attempt to do it here. This list can be established by slightly adapting the proof made for type I twinning in [45], as follows. The twinning direction has to be generated from a two-fold axis [58]. There are nine such directions in the bcc lattice ($\langle 110\rangle_B$ and $\langle 100\rangle_B$) [58], that generate five non equivalent directions in the orthorhombic lattice (calculated with the correspondence matrix of Appendix A), namely $\langle 001\rangle_O$, $\langle 010\rangle_O$, $\langle 100\rangle_O$, $\langle 011\rangle_O$ and $\langle 211\rangle_O$.

The calculation of the twinning elements following the condition of equivalent correspondences shows that a twinning plane does not exist for $\langle 001\rangle_O$, $\langle 010\rangle_O$ and $\langle 100\rangle_O$ (the calculated plane coordinates are (000)). The $\langle 011\rangle_O$ direction corresponds to the so-called compound twinning (meaning both the twinning plane and direction are rational) and is the same as the twinning system B mentioned above and in Table 4. Therefore, only $\langle 2\bar{1}\bar{1}\rangle_O$ remains as a potential direction for type II twinning. The twinning plane and magnitude can then be obtained by adapting the procedure provided for type I twinning in [43]. The expression of the shearing plane in the orthorhombic basis is provided in Table 4.

Experimental observations can help to narrow down the list of possible twinning systems. It appears that, whereas type A twinning and type II twinning have been experimentally reported in the literature to act as LIS modes [28,44,27], type B is generally not observed. This point will be discussed later but, for the time being, we hence exclude type B twinning from the list of potential LIS systems to perform our calculations.

3.1.2. Selection of the potential glide systems

To the best of our knowledge, and as opposed to the case where the LIS is accomplished by twinning, no rules have been reported in the literature to determine which glide systems can act as LIS. Here, the choice of potential glide systems is inferred from the following reasoning. As the inhomogeneous shear is lattice invariant and is assumed to take place in the product phase, the dislocations involved in the process should have lattice translation Burgers vectors in the product lattice. The energy required for the spontaneous formation of a dislocation with said Burgers vector is too high for thermal agitation nucleation within the time and temperature ranges associated to martensitic transformation [59]. Hence, the only available dislocations for the lattice invariant shear will be considered to be those inherited from the parent phase. Dislocations in bcc metals are commonly of $\frac{1}{2}\langle 111\rangle_B$ type [59]. The four equivalent $\langle 111\rangle_B$ directions in the bcc lattice and the directions they generate in the orthorhombic or hcp lattice are shown in Table 5. The bcc dislocations generate two possible non equivalent dislocations in the orthorhombic or hcp lattice that we labelled G and H in Table 5.

Table 5
Possible types of dislocations in the parent and product lattices.

Label	Dislocation in the bcc lattice	Generated dislocation in the product lattices	
G	$\frac{1}{2}[111]_B$	$\frac{1}{2}[\bar{1}01]_O$	$\frac{1}{6}[\bar{2}113]_H$
G	$\frac{1}{2}[11\bar{1}]_B$	$\frac{1}{2}[101]_O$	$\frac{1}{6}[2\bar{1}\bar{1}3]_H$
H	$\frac{1}{2}[\bar{1}11]_B$	$\frac{1}{2}[\bar{1}10]_O$	$\frac{1}{3}[\bar{1}2\bar{1}0]_H$
H	$\frac{1}{2}[1\bar{1}1]_B$	$\frac{1}{2}[\bar{1}\bar{1}0]_O$	$\frac{1}{3}[\bar{1}\bar{1}20]_H$

Dislocations of type H correspond to lattice translation vectors in the orthorhombic and hcp phases whereas dislocations of type G have a Burgers vector corresponding to half a lattice translation vector [60],[3] and their motion in the product phase would thus create stacking faults in their wake. Thus, the shear induced by type G dislocations is not lattice invariant, and these dislocations are discarded. As a result, type H dislocations ($\frac{1}{3}\langle\bar{1}2\bar{1}0\rangle_H$ or $\frac{1}{2}\langle\bar{1}10\rangle_O$) are expected to be those involved in the lattice invariant shear. It remains to determine what are the possible glide planes for these dislocations. We assume that the LIS systems should be selected among the slip systems usually observed during conventional plastic deformation. A list of the experimentally reported slip systems in the hcp phase of titanium alloys has been reported in [48]. In this list, only three families of glide systems involve type H dislocations. They have been gathered in Table 6, and labelled H1, H2 and H3. We assume that they are the most plausible candidates for the lattice invariant shear. Among these three possible slip systems, only H1 and H2 can act as LIS systems for Ti alloys, because for the system H3, the restriction on the plane (Eq. (2)) cannot be fulfilled simultaneously with the restriction on the direction (Eq. (3)) for the range of eigenvalues displayed by Ti alloys. It should be noted that the argumentation described above does not lead to the same glide systems as the ones usually considered for titanium alloys, that come from Otte's work [48]. The discrepancy between the list of this work and Otte's will be discussed later. As opposed to the cases where the LIS is produced by twinning, where the twinning systems are usually well characterized, experimental characterization of both the shear plane and direction involved in the LIS is rare when martensite is not internally twinned. We therefore cannot use experimental reports to narrow down the list of glide systems, as has been done above for twinning systems, and we will consider hereon that both systems H1 and H2 are plausible candidates to accomplish the LIS.

3.1.3. Summary

A set of two glide systems and two twinning systems are selected as candidates to accomplish the lattice invariant shear. These systems are listed in Tables 7 and 8, with the coordinates of the planes

[3] Indeed, lattice translation vectors in the hcp lattice are given by $k[x_1, x_2, x_3, x_4]_H$, with $k = \frac{1}{3}$ if $(x_1 - x_2)$ is a multiple of 3, and $k = 1$ otherwise [60]

Table 6
Glide systems of the orthorhombic or hcp phase involving $\frac{1}{2}\langle\bar{1}10\rangle_O$ dislocations.

Label	hcp	orthorhombic	bcc
H1	$(0001)_H\ \frac{1}{3}[1\bar{2}10]_H$	$(001)_O\ \frac{1}{2}[1\bar{1}0]_O$	$(110)_B\ \frac{1}{2}[1\bar{1}\bar{1}]_B$
H2	$(10\bar{1}1)_H\ \frac{1}{3}[1\bar{2}10]_H$	$(111)_O\ \frac{1}{2}[1\bar{1}0]_O$	$(01\bar{1})_B\ \frac{1}{2}[1\bar{1}\bar{1}]_B$
H3	$(10\bar{1}0)_H\ \frac{1}{3}[1\bar{2}10]_H$	$(110)_O\ \frac{1}{2}[1\bar{1}0]_O$	$(\bar{1}1\bar{2})_B\ \frac{1}{2}[1\bar{1}\bar{1}]_B$

Table 7
Possible lattice invariant shear systems; coordinates of the shear planes in the eigenbase.

	Shear plane in the eigenbase (h_1, h_2, h_3)
Twinning A	$\frac{1}{2}(\sqrt{2}, \bar{1}, \bar{1})_P$
Twinning II	$\left(\eta_2^2+\eta_3^2-2\eta_1^2, \frac{3\eta_2^2-\eta_3^2-2\eta_1^2}{\sqrt{2}}, \frac{-\eta_2^2+3\eta_3^2-2\eta_1^2}{\sqrt{2}}\right)_P$
Glide H1	$(001)_P$
Glide H2	$\frac{1}{2}(\sqrt{2}, 1, 1)_P$

and directions expressed in the eigenbase, so that the values can directly be input to Eqs. (2) and (3). Comparison with experimentally observed planes will be discussed later.

4. Identification of the compositional space where martensite formation is possible from a crystallographic point of view

Now that a list of plausible lattice invariant shear systems is proposed, the conditions expressed by Inequations (2) and (3) allow to determine whether martensitic transformation is possible with a certain LIS depending on the lattice parameters.

4.1. Transformation compositional restrictions

The restrictions on the planes and directions allow to define eigenvalue ranges where the transformation is possible. For each LIS system, the limits in "eigenvalue space" indicate the ranges within which martensitic transformation is possible. For example, for type A twinning (Table 7), the restriction on the LIS plane expressed by inequation (2) allows to define a surface in (η_1, η_2, η_3) space, described by the following equation:

$$\frac{1}{2}\cdot(1-\eta_2^2)\cdot(1-\eta_3^2)+\frac{1}{4}\cdot(1-\eta_3^2)\cdot(1-\eta_1^2)+\frac{1}{4}\cdot(1-\eta_1^2)\cdot(1-\eta_2^2)=0 \quad (5)$$

and represented by the blue surface in Fig. 4 and expanded in Appendix B. Martensitic transformation with type A twinning is impossible on the left hand side of the blue surface. Similarly, the restrictions on the LIS direction expressed in Inequation (2) allow to define a surface in (η_1, η_2, η_3) space, described by the following equation:

$$\begin{aligned}&(4\eta_2^2\eta_3^2-2\eta_2^2\eta_1^2-2\eta_3^2\eta_1^2)^2\cdot\eta_1^2\cdot(1-\eta_2^2)\cdot(1-\eta_3^2)\\&\quad+2\cdot(2\eta_2^2\eta_3^2+2\eta_2^2\eta_1^2-3\eta_3^2\eta_1^2)^2\cdot\eta_2^2\cdot(1-\eta_1^2)\cdot(1-\eta_3^2)\\&\quad+2\cdot(2\eta_2^2\eta_3^2-3\eta_2^2\eta_1^2+\eta_3^2\eta_1^2)^2\cdot\eta_3^2\cdot(1-\eta_1^2)\cdot(1-\eta_2^2)=0\end{aligned} \quad (6)$$

and represented by the yellow surfaces in Fig. 4. Eq. (3) is met in the region between the two yellow surfaces. When the LIS occurs due to twinning, the twinned fraction cannot exceed 1. The surface $f_{tw}=1$ is plotted as a red surface in Fig. 4.[4] The region where all conditions for martensitic transformation are met is labelled R1 in Fig. 4.

[4] It can be shown that in the usual range of eigenvalues for binary titanium alloys, for type A twinning, the necessary twinned fraction exceeds 1 or is lower than 0 if the third eigenvalue is less than unity.

Vectors showing the variation of the eigenvalues when alloying elements are added to pure Ti are shown in Fig. 4 for the bcc to orthorhombic transformation. Each bullet represents an increase of 1 at% in the given alloying element, and the red star shows the eigenvalues associated with the transformation of pure titanium. For pure titanium and low solute contents, where the orthorhombic phase is normally not observed, trends have been extrapolated. As alloying elements are added, as symbolized on the map by arrows, the points move away from pure titanium towards surfaces and may eventually cross them to reach a zone where the transformation is impossible. The map shows, for example, that for the Ti-Mo system, martensitic transformation is possible with type A twinning until its vector crosses the blue surface, which corresponds to Ti-14Mo (wt%). For higher concentrations, twinning A does not allow the transformation to take place. A similar plot for the eigenvalues associated to the bcc to hcp martensitic transformation in three binary systems is shown in Appendix B. Additionally, similar surfaces can be drawn for type II twinning and for the two potential glide systems Appendix B. This allows to calculate, for each binary system, the range of compositions for which martensitic transformation is crystallographically allowed.

4.2. Summary and comparison to experiments

The possibility to form martensite with one or the other LIS system as a function of composition, calculated as exposed above, is shown in Figs. 5 and 6 together with the experimentally reported behaviour regarding martensitic transformation. It can be noted that the experimental compositions at which martensite forms sometimes slightly overlap with those at which martensite is inhibited, due to the experimental results being collected from different sources. The calculations were performed for α' in Ti-Fe, Ti-Cr and Ti-Zr, because these systems are known to display only hcp martensite; and for α" for the other systems. The experimentally observed concentrations above which martensite is not observed match fairly well the calculated thresholds for which the geometry of the lattices does not allow an IPS to accomplish the transformation. For orthorhombic systems, the calculations indicate that no martensite can form above 14 wt% in Ti-Mo, 17 wt% in Ti-V, 37 wt% in Ti-Nb and 78 wt% in Ti-Ta (Fig. 5), which is relatively consistent with experiments. The calculations also show that martensite can crystallographically form in any mixture of Ti and Zr (Fig. 6), which is also consistent with experiments. Some systems, such as Ti-Ta, Ti-Nb (Fig. 5) and Ti-Os (Fig. 6) display different critical concentrations depending on the LIS system, whereas others, such as Ti-Fe, Ti-Cr (Fig. 6), Ti-Mo or Ti-V (Fig. 5) exhibit a single compositional threshold for all considered LIS systems. These common thresholds can be explained by the fact that, at a certain concentration, Ti-Fe, Ti-Cr, Ti-Mo and Ti-V reach $\eta_3 = 1$ (i.e. the horizontal planes on Fig. 4, which corresponds to a common border for the four LIS systems).

5. Computation of the Ms temperature

The procedure described above outlines a necessary condition for martensite formation; at least one LIS system should allow for geometric accommodation via an IPS. However, for the transformation to take place, crystallographic feasibility must be accompanied by a system energy reduction. A way to verify whether martensite is stable at room temperature is to calculate its martensite start temperature (M_s). A model for this has been proposed in [25]. However, in such procedure the elastic strain energy was calculated without accounting for the orientation of the habit plane. The determination of the geometric elements of the transformation, as expressed here, allows for a more precise calculation. To obtain the elastic strain energy due to an invariant plane strain P_m, the total displacement vector m $\mathbf{d_m}$ can be decomposed into a uniaxial dilatation $\mathbf{d_u}$

Table 8
Possible lattice invariant shear systems; coordinates of the shear directions in the eigenbase.

	Shear direction in the eigenbase $[u_1, u_2, u_3]$
Twinning A	$[4\eta_2^2\eta_3^2 - 2\eta_2^2\eta_1^2 - 2\eta_3^2\eta_1^2,\ \sqrt{2}\cdot(2\eta_2^2\eta_3^2 + \eta_2^2\eta_1^2 - 3\eta_3^2\eta_1^2),\ \sqrt{2}\cdot(2\eta_2^2\eta_3^2 - 3\eta_2^2\eta_1^2 + \eta_3^2\eta_1^2)]_P$
Twinning II	$\frac{1}{2}[\sqrt{2}, \bar{1}, \bar{1}]_P$
Glide H1	$\left[\frac{\bar{1}}{\sqrt{3}}, \sqrt{\frac{2}{3}}, 0\right]_P$
Glide H2	$\left[\frac{\bar{1}}{\sqrt{3}}, \sqrt{\frac{2}{3}}, 0\right]_P$

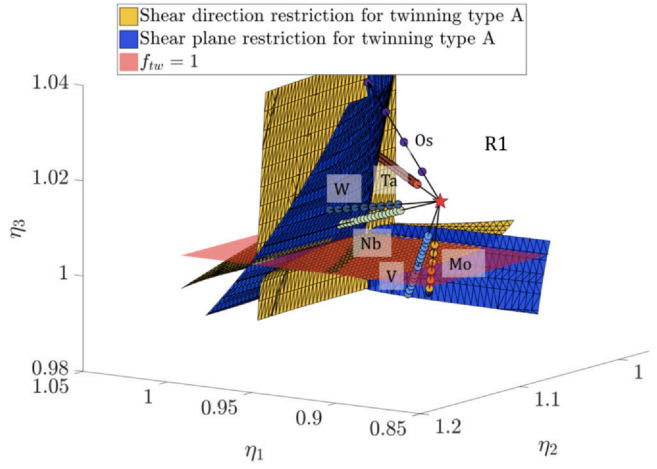

Fig. 4. Limits for the martensitic transformation to be possible with twinning of type A as LIS, together with eigenvalues for orthorhombic martensitic transformation in some binary Ti-x systems. These binary systems are those for which martensite is known to be orthorhombic above a certain concentration. The plain black lines represent the extrapolation of the eigenvalues for concentrations for which orthorhombic martensite does not exist (pure Ti and dilute alloys), and each bullet represents an increase of 1 at% in the given alloying element.

(parallel to the normal to the habit plane $\mathbf{p_m}$, where $\mathbf{p_m}$ is a unit vector) and a shear component $\mathbf{d_s}$ lying in the habit plane. Once P_m is determined, this decomposition is straightforward ($\mathbf{d_u} = m(\mathbf{p_m}'\mathbf{d_m})\,\mathbf{p_m}$ and $\mathbf{d_s} = m\,\mathbf{d_m} - \mathbf{d_u}$ if the vectors are expressed in an orthonormal basis). From Eshelby's theory, Christian derived the expression for the volumetric elastic strain energy E_{el} of such a transformation for an ellipsoidal plate of semi-thickness c and radius r [62]:

$$E_{el} = \frac{\mu}{1-\nu}\cdot\frac{\pi}{4}\cdot\frac{c}{r}\left(d_u{}^2 + \frac{(2-\nu)}{2}d_s{}^2\right) \tag{7}$$

where μ is the shear modulus of the considered alloy and ν its Poisson ratio. The total change in energy associated with the transformation is $\Delta G = \frac{4}{3}\pi r^2 c\,(E_{el} - \Delta G^{ch}) + 2\pi r^2\gamma$ where ΔG^{ch} is the volumetric chemical driving force for the transformation and γ is the interfacial energy. Then, a martensite plate of semi-thickness c_d and radius a is in thermo-mechanical equilibrium with its surroundings when $\left(\frac{\partial \Delta G}{\partial c}\right)_{c=c_d} = 0$:

$$\Delta G^{ch}(T) = 2\cdot\frac{\mu(T)}{1-\nu}\cdot\frac{\pi}{4}\cdot\frac{c_d}{a}\left(d_u{}^2 + \frac{(2-\nu)}{2}d_s{}^2\right) \tag{8}$$

In Eq. (8), ΔG^{ch} is approximated with that of the $\beta \rightarrow \alpha$ transformation, this approximation has been discussed in [24,25]. ΔG^{ch} is computed using the "TCTI1" database of Thermo-Calc® software. μ depends on temperature and composition, as stated in [63], and d_s and d_u depend on composition via the lattice parameters as detailed in Section 3. M_s is considered to be the temperature at which a martensite plate of 50 nm semi-thickness and 100 μm diameter is in thermomechanical equilibrium with its environment (as in [25]). This temperature is obtained by iteratively computing the elastic strain energy and the chemical driving force for different temperatures until Eq. (8) is met. The elastic strain energy associated with the presence of a martensite plate depends on the magnitude of the macroscopic deformation P_m, and thus on the chosen LIS systems. Therefore, several M_s temperatures can be calculated, one for each geometrically possible LIS. An example of M_s calculation is displayed in Fig. 7 along with the temperature T_0, defined as the partitionless equilibrium temperature between the hcp and bcc phase. The M_s calculations are illustrated for Ti-Cr and Ti-Fe binary systems, as these systems are known to form martensite only upon quenching, which makes comparison with experimental M_s more straightforward. For comparison purpose, the M_s that would be obtained if the transformation occurred without a LIS is also shown in Fig. 7; the procedure to calculate it is detailed elsewhere [25]. It can be noticed in Fig. 7 that the scatter between the calculated M_s corresponding to different LIS systems is very small, and that all the calculated M_s are very close from T_0, indicating that the elastic strain energy only has a minor contribution on the M_s temperature.

While the geometric behaviour may exhibit discontinuities with respect to composition, it can be seen with the calculation of T_0 that there is no discontinuity in the thermodynamic stability of the hcp phase, since T_0 gradually decreases upon chromium or iron addition, and is still far above room temperature at compositions for which martensite is never reported. This seems to indicate that the sharp transitions observed on the martensitic behaviour of Ti alloys are due to geometric compatibility issues, and cannot be solely explained by the thermodynamic stability of the different phases. It is sometimes claimed that the critical composition from which martensite stops forming is the composition at which the M_s temperature falls below room temperature, which is inconsistent with the present calculations, both from thermochemical and micromechanical points of view. As a matter of example, Otte [64] noticed that martensite did not form in a Ti-10Cr alloy, even when quenched down to −196 °C. As he pointed out, any reasonable extrapolation of the known M_s in this binary system would have made one expect the M_s temperature to lie around 200 °C. On the other hand, the arguments related to crystallography presented here can explain this observation.

6. Discussion

6.1. Choice of the possible inhomogeneous shear or twinning systems

The PTMC requires to choose potential inhomogeneous shear systems, but there is no general agreement on which systems are activated in Ti alloys, and no clear rule exists to make such a choice. It is not the focus of this work to explain the choice of the activated, but rather to establish a list of systems that seem to be plausible candidates to realise the LIS. In order to validate our initial hypothesis, it is necessary to verify whether the list of LIS systems determined here (Tables 7 and 8) is consistent with experimental observations.

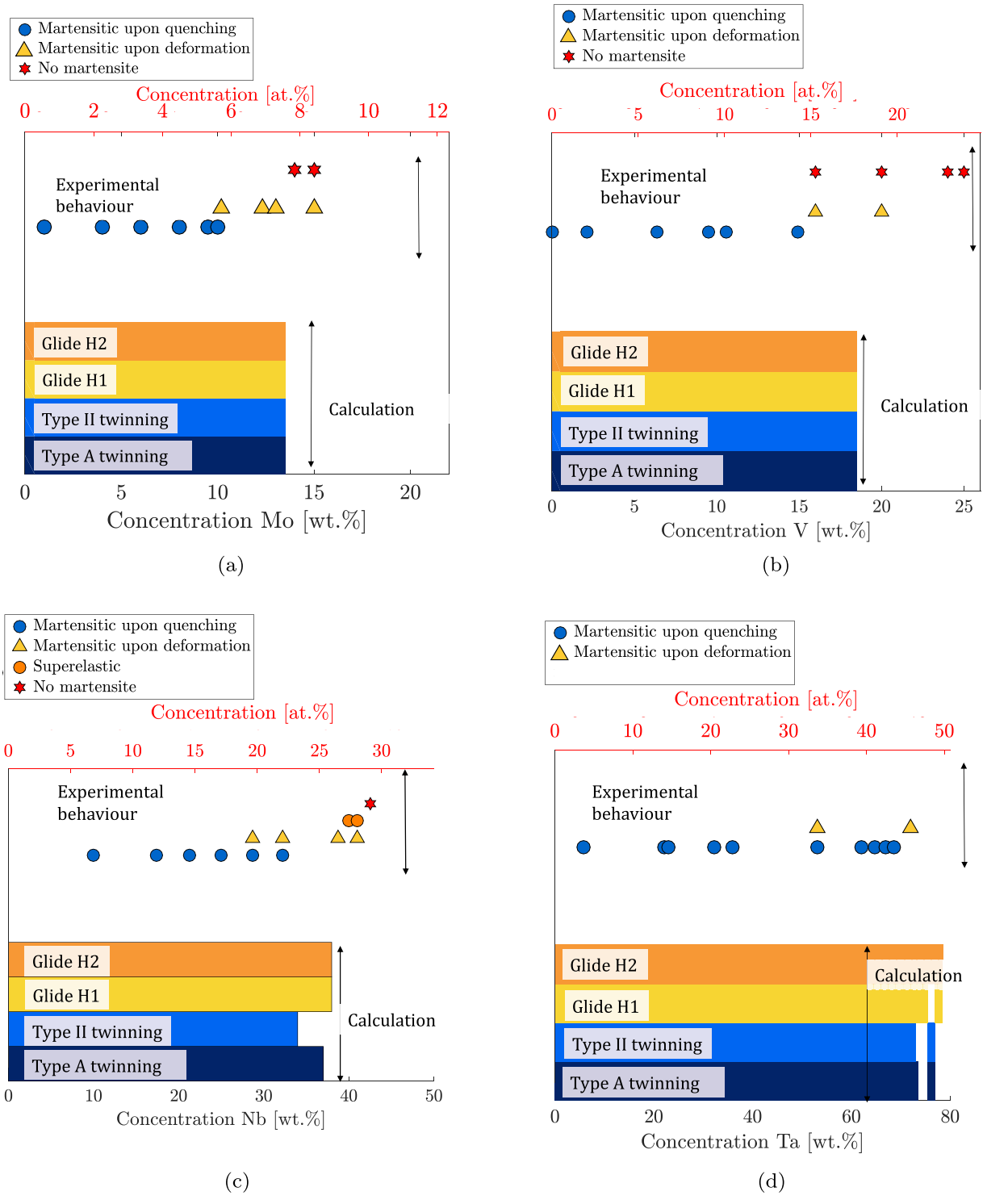

Fig. 5. Possibility to form α" martensite with the four potential LIS systems as a function of composition in binary systems. The experimental observations are collected from [22,35,14,36,13] for Ti-V, [22,15,37,14,16] for Ti-Mo, [17,28] for Ti-Ta and [38,21,39,40] for Ti-Nb. Superelasticity corresponds to martensite formation upon loading which reverses to the parent phase upon unloading.

6.1.1. Choice of potential twinning systems

The present work leads to the conclusion that type A and type II twinning modes are the most likely to be activated, whereas type B is discarded. The conclusion that type B twinning does not act as a LIS system agrees with a large body of experimental evidence. First, in most cases where martensite forms, type B twinning is anyway not allowed due to the restrictions on the shear plane and direction (Eqs. (2) and (3)). It has also been reported that in some special conditions where the lattice parameters would make it possible for this system to act as LIS, this twinning mode was not activated [31,65,27]. Nevertheless, Williams et al. observed type B twins in some Ti-Cu alloys [66], and such twins have also been reported in Ti alloys containing Ag and Mg [31], which may seem in contradiction with our conclusion that type B twinning should not act as a LIS mode. However, Williams et al. [66] claimed that the type B twins they observed in Ti-Cu were most likely induced by the stress

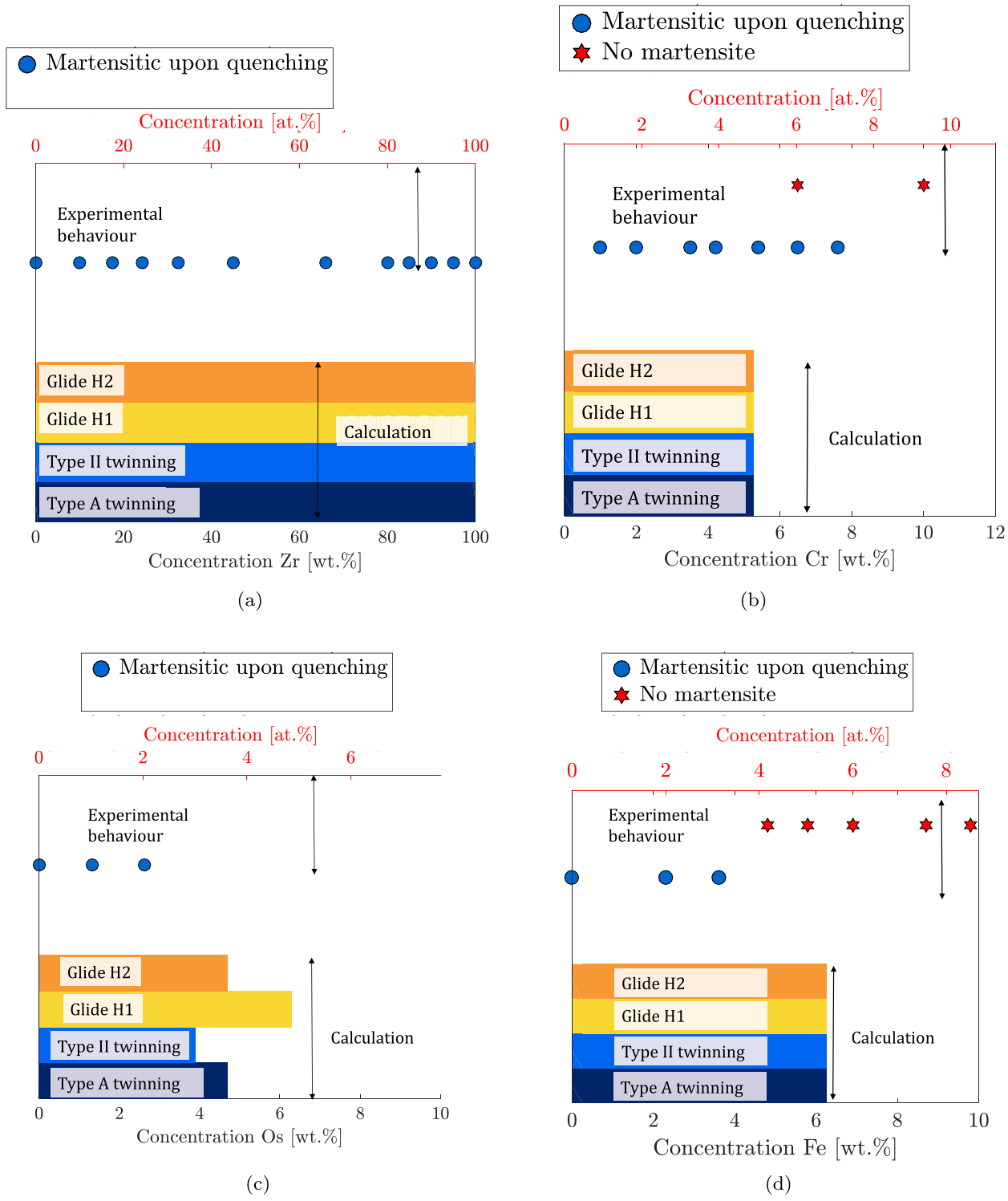

Fig. 6. Possibility to form martensite with the four potential LIS systems as a function of composition in binary systems. The experimental observations are collected from [11] for Ti-Fe, [17,61,33] for Ti-Cr, and [22] for Ti-Os. The calculations were performed for α' martensite for Ti-Fe, Ti-Zr and Ti-Cr, as these systems do not display any orthorhombic martensite; and for α" for Ti-Os.

resulting from the formation of secondary martensite plates. Banerjee et al. [67], who observed type B twins in a zirconium alloy, reached the same conclusion. Thus, we suggest that the occasional presence of type B twins in martensite is not inconsistent with our conclusion, and we infer that whenever such twins are observed, they should be resulting from the stress associated with the formation of new plates rather than from the necessary LIS.

Nevertheless, the absence of type B twinning as a lattice invariant shear mode is not always well explained, especially considering that it has recently been reported as a deformation twinning mode in a Ti-Mo alloy [68]. It is not clear why this twinning mode, which involves the smallest shear among all possible hcp twinning modes, and a reasonable shuffle [69], can act as mechanical twinning mode, but is usually not observed as a transformation twinning mode, even

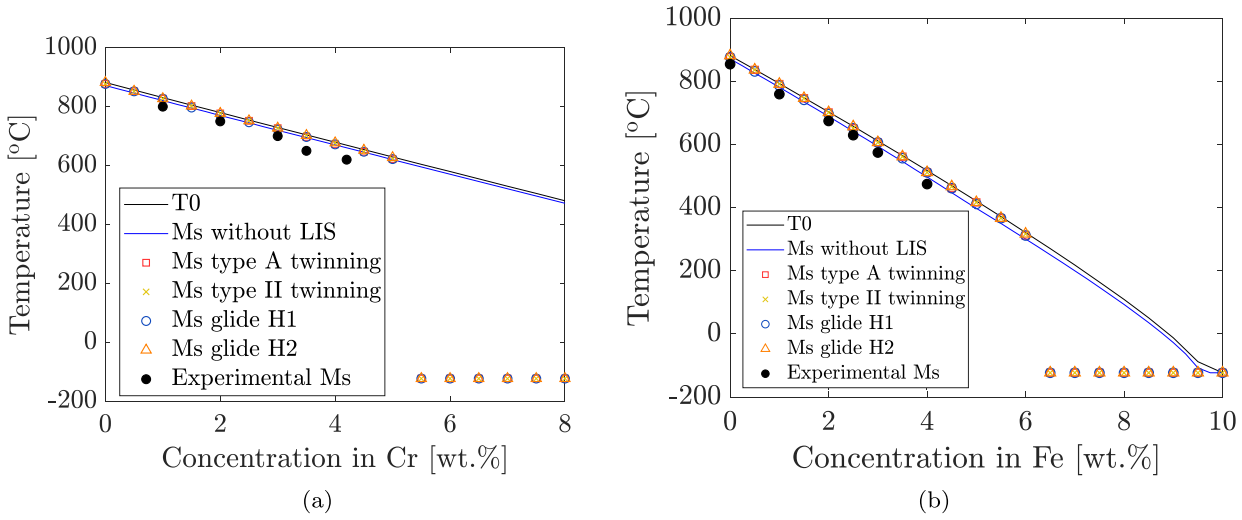

Fig. 7. Example of calculation of the M_s temperature in Ti-Cr an Ti-Fe. The black bullets show the experimental M_s from [23,35]. Whenever the transformation is "crystallographically impossible" with a given LIS system, the M_s was arbitrarily set to −120 °C.

in conditions where the lattice parameters would allow it. Sun *et al.* proposed an explanation based on calculations of the critical shear stress for twinning and concluded that the order of magnitude of the critical shear stress for type B twinning was approximately six times higher than the critical shear stress for type A twinning [31], which may constitute an explanation for the usual absence of type B twinning as a LIS mode. Further work would be needed to relate the critical stress for the activation of all LIS modes to the composition, in order to verify that type B twinning is less energetically favourable than any of the other modes proposed here.

Conversely, twinning systems A and II as possible LIS modes constitue a reasonable choice since both have been widely reported. Type A transformation twins were observed in pure Ti [70] and in a number of alloys including Ti-V [71], Ti-Ta [28], Ti-Mo [72], Ti-Nb [29], Ti-Nb-Al [27], Ti-Mn [15,73], and Ti-Cr [18,74]. There are fewer reports of type II transformation twins but, as pointed out in [47,28], type A and type II twins can be easily confused, and this mode of LIS has at least been reported in Ti-Ta [28] and Ti-Nb-Al [27] alloys. Therefore, the choice of type A and II as the only possible LIS twinning modes is well supported by the literature.

6.1.2. Choice of potential glide systems

Investigations of PTMC in titanium alloys often focus on twinning only as the LIS mode [27,45]. It is however of interest to consider not only twinning but also glide as a potential LIS mechanism. Indeed, internal twins are not systematically observed in martensite, and it has been experimentally confirmed that the LIS can take place by dislocation glide [28]. However, the complete characterization of the involved LIS systems is experimentally complex and hence rare. In this work, two glide systems were retained as potential LIS systems, relying on theoretical considerations (Section 3.1.3). Although there is little experimental support for their choice, we attempt to show here that our choice is not in disagreement with experiments.

It was postulated here that only $\frac{1}{3}\langle 11\bar{2}0\rangle_H$ dislocations could be involved in the LIS. These dislocations have indeed been observed in martensite plates in Ti-Mo [72], Ti-Cu [66] and Ti-V [71]. In the present work, $\frac{1}{3}\langle\bar{2}113\rangle_H$ (labelled G) dislocation glide as LIS was considered as unlikely, since these dislocations cannot be generated from simple dislocations from the parent phase (two bcc dislocations would be necessary to generate one $\frac{1}{3}\langle\bar{2}113\rangle_H$). This seems in disagreement with observations made in some Ti-Cu alloys [66] and Ti-V alloys [71], where $\frac{1}{3}\langle\bar{2}113\rangle_H$ dislocations were reported as interface dislocations. However, in both cases, these observations were made on plates where multiple LIS systems were activated and where at least one of the LIS systems considered in Table 7 was activated as well. We suggest that in those cases, the operating LIS mode is among the ones proposed here, and that the presence of $\frac{1}{3}\langle\bar{2}113\rangle_H$ dislocations at the interface may be the consequence of the accommodation stresses. The choice of the potential glide planes is more difficult to verify, since even when dislocations are identified in martensite, there are very few reports on the planes on which they lie. In the few cases where the entire LIS glide mode was described, however, the results are consistent with the conclusion reached here. In Zr-Ti alloys, for example, Banerjee et al. observed dislocations in a plane that corresponds to the H2 system described in Table 7. Therefore, the assumptions made here regarding the potential LIS glide systems show no inconsistency with reported experimental results, although it should be kept in mind that only a detailed experimental characterization of LIS modes would fully confirm them. There is no evidence that all of the chosen shear systems can indeed act as LIS, even in conditions where the geometry makes it possible. The calculations presented here are led by considering the systems that *can* constitute LIS, which does not mean that all of them are active.

6.1.3. Comparison with other attempts from the literature to determine the inhomogeneous shear systems

To our knowledge, the only attempt to systematically investigate the theoretically possible LIS systems in Ti alloys is the one performed by Otte [48]. The conclusions drawn by Otte contrast with our findings, since the two systems considered by him as the most probable ones (glide along $[2\bar{1}\bar{1}3](\bar{2}112)$ and $[2\bar{1}\bar{1}3](\bar{1}011)$) are not in the list considered here. To determine which systems are the most likely, Otte calculated the coordinates of the habit planes associated with a number of plausible glide and twinning systems as LIS, and adopted the ones that allowed best agreement with reported experimental habit planes. Although his method is very reasonable, the results are somehow in disagreement with experiments, since they led him to conclude that type A and type II twinning are not likely to act as LIS systems, although these modes have been unambiguously characterised as LIS modes in numerous titanium alloys (Section 6.1). Considering the large uncertainty on the habit plane measurements along with the sensitivity of the habit plane calculations to the lattice parameters (detailed below), it was chosen in this work not to primarily focus on agreement between habit plane

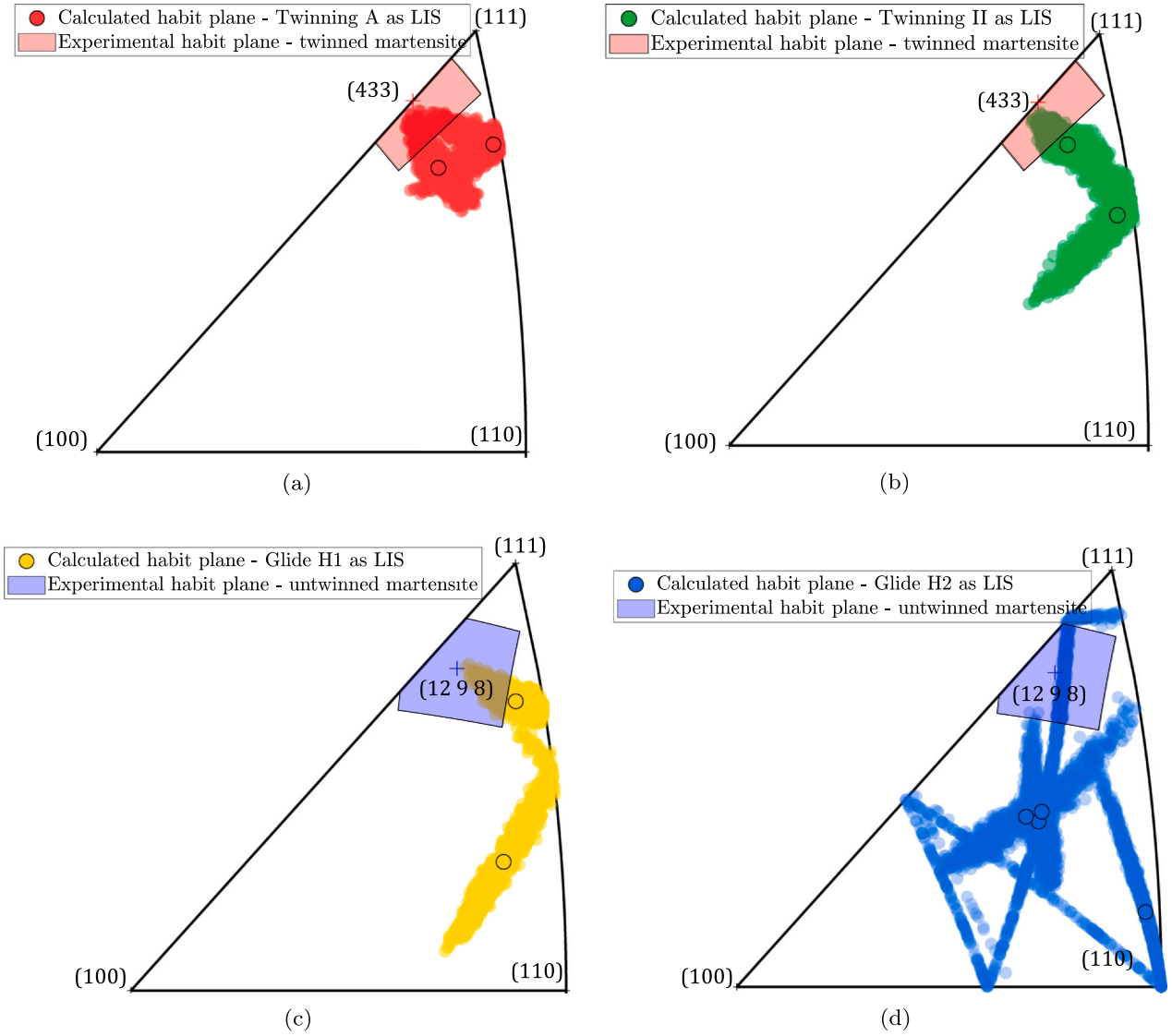

Fig. 8. Stereographic projections of calculated habit planes for various LIS systems in pure titanium; (a) type A twinning (b) type II twinning (c) glide with H1 system (d) glide with H2 system. The black circled bullets represent the habit plane coordinates computed with the lattice parameters as described above. The cloud of points (1000 per system) represents the calculation results when randomly varying the lattice parameters in the range ± 0.015 Å around the initial calculated value. Experimental habit planes observed for internally twinned martensite ((a) and (b)) and untwinned martensite ((c) and (d)) are also displayed. The red and blue zones around the experimental habit planes represent an uncertainty of 5° around the announced habit plane.

calculations and measurements to infer a list of plausible LIS systems, but rather to give more importance to geometric considerations, and to experimental characterization of LIS systems when available. Moreover, as detailed below, the choice of LIS systems made in the present work is still consistent with reported habit planes measurements.

6.1.4. Comparison between experimental and calculated habit planes

The coordinates of the habit planes depend on the activated LIS system. Thus, a comparison between experimental measurements and calculations of habit planes coordinates may help confirming or discarding the list of LIS systems. The uncertainty is in general significant on experimental values of habit plane coordinates due to the large scatter generally observed in the measurements [75–77], and to the fact that the reported coordinates are usually not those of the centre of the cluster of experimental measurements, but rather those of the closest lattice plane. An uncertainty of 5° on these measurements is therefore assumed here, consistently, for example, with the scatter exhibited by the measurements of [75] or [77]. The uncertainty on habit plane calculation performed with the PTMC can be large as well, mainly because of the uncertainty on the lattice parameters calculation, which is estimated here to ±0.015 Å for reasons exposed later (Section 6.2). The comparison between measured habit planes coordinates and calculations performed with the list of LIS systems described above for α' is exemplified in Fig. 8 in the case of pure titanium. In pure titanium, both twinned martensite with $\{334\}_B$ habit plane [70] and non-twinned martensite with $\{12, 8, 9\}_B$ habit plane [78] have been reported. The stereographic projections of these experimental habit planes are displayed with an uncertainty of 5° in Fig. 8a and b for the former, and in Fig. 8c and d for the latter. The calculated habit planes, taking into account the uncertainty on the lattice parameters, are also shown in Fig. 8. The uncertainty on the lattice parameters were taken into account by executing each habit plane calculation 1000 times, varying randomly

the lattice parameters in the range ± 0.015 Å around the initial calculated value. Although the scatter is very large, the calculations are consistent with observations. In turn, in the case of twinned martensite, the activation of type A or type II twinning as LIS may equally explain the observed $\{334\}_B$ habit plane (in reality, only type A transformation twins were reported [70] to our knowledge, but as mentioned before, type II is not to be neglected as it has already been reported to act as transformation mode). In the case of the $\{12, 8, 9\}_B$ habit plane, no transformation twins were observed, which means that the LIS should occur by dislocation glide, but no experimental information was found in the literature regarding the activated glide system. As shown in Fig. 8, both H1 and H2 systems may explain the observed habit planes. It should be noted that, given the large uncertainty on both habit plane measurements and calculations, agreement between both does not appear to be sufficient to infer which system is activated. This does however constitute a supplementary evidence that the selection of LIS made here is consistent. Similar comparisons between habit plane calculations and experiments were performed for a variety of alloys where the habit planes were characterised, and where martensite was reported not to be internally twinned; namely Ti-53Ta [28], Ti-5V [71], Ti-16Nb-3Al (at%), Ti-18Nb-3Al(at%)[5][27] and Ti-20Nb (at%) [29]. It turned out that, in each of these cases, the experimental observations can be explained by activation of system H1, system H2 or both, provided the uncertainties are taken into account. Thus, the choice of LIS systems made here is further supported by a reasonable agreement between experimental and calculated habit planes.

6.2. Sensitivity of the model to lattice parameters

The approach proposed here is sensitive to the lattice parameters. Those used for calculations are derived from linear functions of the concentration in alloying elements, which coefficients are extracted from measurements reported in the literature. The precision of the calculated values is limited due to the experimental uncertainty on the measurement (generally between around ± 0.005 Å and ±0.01 Å [50,72]), the uncertainty in the linear relationship that is assumed, or the fact that the lattice may be able to elastically contract or expand to reach dimensions promoting the transformation.[6] Yan et al. analyzed the lattice parameters for three binary systems coming from multiple sources from the literature [50]. From their data, it appears that the usual maximum difference between lattice parameters measurements performed by different authors for the same composition is around 0.03 Å. This scatter should include the errors coming from the sources listed above. Therefore, in order to evaluate the sensitivity of the present calculations to the lattice parameters, the thresholds above which martensite is not supposed to form were recalculated by changing the lattice parameters values within a reasonable range. The calculations were performed a thousand times for each binary system, and for some ternary systems (varying the concentration in one element), adding every time random values in the range [−0.015 Å, +0.015 Å] to all lattice parameters. For each set of calculations, β_d was determined as the lowest concentration for which crystallographic accommodation is impossible. This allows to determine a domain where 95% of the calculated β_d are located. Fig. 9 displays the results of these calculations as a function of the experimental observations regarding these systems, where the reported experimental ranges are also represented. The sensitivity of the calculations to the lattice parameters is of the same order than the experimental scatter. Thus, even considering a potential error of ± 0.015 Å on the estimation of the lattice parameters, the method presented here allows to explain fairly well the absence of martensite in Ti alloys, or at least to rank the addition elements by their martensite inhibition power. In summary, although an error on the lattice parameters would modify the calculated thresholds above which martensite cannot form, the trends remain correct, and the PTMC allows to explain or interpret the inhibition of martensite above critical values of element concentrations.

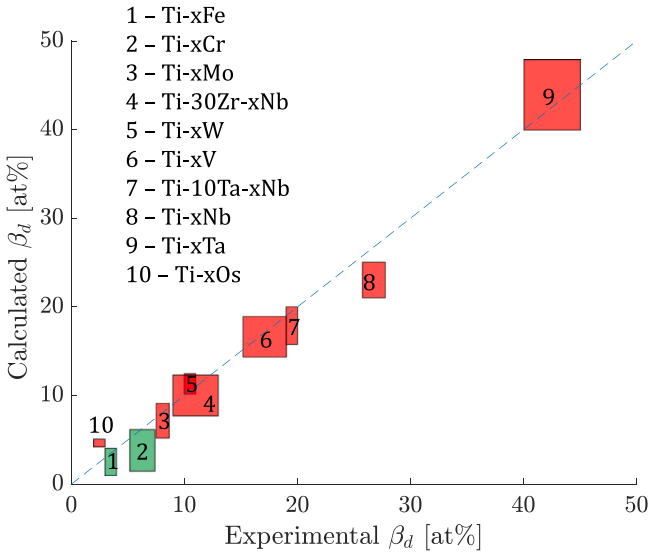

Fig. 9. Comparison between the experimental thresholds above which martensite is not observed and the calculated thresholds. The height of the boxes represents the uncertainty in the calculation when varying the lattice parameters ± 0.015 Å, whereas the width of the boxes represent the possible critical compositions, according to experimental observations extracted from the literature. Green boxes are for hcp structure, red boxes for orthorhombic structure. The upper bounds of experimental thresholds for Ti-W and Ti-Ta are speculated; indeed, Ti-W alloys have been reported to display martensite upon quenching up to 10 at% and Ti-40Ta has been reported to form martensite upon deformation, but no information was found regarding higher concentrations in W or Ta.

6.3. Crystallographic interpretation of transitions regarding martensitic transformation

Different reasons are mentioned in the literature regarding the suppression of martensite formation (even upon deformation) in concentrated alloys. As mentioned before, the hypothesis that martensite formation is suppressed in β alloys because the M_s temperature becomes too low is not convincing, since the thermodynamic driving force for martensite formation is very high at concentrations where martensite is not observed (Fig. 2). Another widespread explanation for the absence of martensite is the presence of ω phase, that would inhibit martensite formation [8]. It is indeed well established that ω phase is often present when martensite is not, which naturally leads to explain the absence of martensite by the presence of ω. However, Cai et al. showed that the ω phase can continuously transform into martensite α" upon deformation in a β metastable alloy [80]. It was also shown in a Ti-Mo alloy that both martensite and ω can form upon deformation in the same sample [81]. It is therefore difficult to assert that the ω phase is on its own responsible for the absence of martensite, even after deformation. Although it is entirely plausible that above a critical fraction of ω phase, martensite cannot form anymore, the present work suggests that the inhibition of martensite is more likely to be due to crystallographic incompatibility.

[5] In that case, the calculations were performed by varying the lattice parameters around the values experimentally reported by Inamura et al. [27] since the dependency of the lattice parameters to the Al content is not known.

[6] Taking a typical ratio between the yield stress σ_y and the elastic modulus E yielding $\frac{\sigma_y}{E} = 4{\cdot}10^{-3}$ [79] and roughly approaching the maximum elastic elongation ϵ by $\epsilon = \frac{\sigma_y}{E}$, the maximal order of magnitude of the error made on the lattice parameters, if they can elastically extend, should be around ±0.01 Å.

7. Conclusions

- Four lattice invariant shear (LIS) systems are thought to be plausible candidates for martensite accommodation in titanium alloys; namely (i) twinning in the $(1\bar{1}\bar{1})_O$ plane (type A) or (ii) in the $[2\bar{1}\bar{1}]_O$ direction (type II), or dislocation glide along either (iii) the $\frac{1}{2}[1\bar{1}0]_O$ direction in the $(001)_O$ plane (H1 system) or (iv) the $\frac{1}{2}[1\bar{1}0]_O$ direction in the $(111)_O$ plane (H2 system). The proposed list of LIS systems is consistent with existing experimental characterisation of LIS systems as well as of habit plane coordinates.
- Martensite inhibition beyond critical concentrations in binary titanium alloys may be explained by the impossibility to transform via any plausible invariant plane strain (IPS). This is demonstrated by extrapolating PTMC calculations to compositions where martensite does not exist.
- A formulation combining computational thermodynamics with the PTMC describes the occurence of martensite formation and the M_s temperature as a function of composition in binary and in some ternary alloys, showing good agreement with the literature.

CRediT authorship contribution statement

Madeleine Bignon: Formal analysis, Validation, Visualization. **Emmanuel Bertrand:** Software, Supervision. **Pedro E.J. Rivera-Diaz-del-Castillo:** Funding acquisition, Supervision, Conceptualization. **Franck Tancret:** Funding acquisition, Supervision, Conceptualization.

Declaration of Competing Interest

The authors declare that they have no known competing financial interests or personal relationships that could have appeared to influence the work reported in this paper.

Acknowledgment

The work of MB has been supported by DGA (French Ministry of Defense). PEJRDDC is grateful to the Engineering and Physical Sciences Research Council U.K. for the provision of funding via grant EP/L025213/1 (Designing Alloys for Resource Efficiency), and to the Royal Academy of Engineering for funding his chair.

Appendix A. Correspondence matrices and basis

In what follows, the considered variant of martensite is related to the parent bcc lattice by the correspondence matrix ${}_BC_O$:

$$ {}_BC_O = \begin{pmatrix} 0 & \bar{1} & 1 \\ 0 & 1 & 1 \\ \bar{1} & 0 & 0 \end{pmatrix} \tag{A.1} $$

which is in accordance with the Burgers relationship [82]. The subscript O is used for the matrices and vector expressed in the orthorhombic basis, and can refer to an orthorhombic or an hcp lattice. Following Bowles and Mackenzie's notation, a column vector which coordinates are expressed in any basis A will be designated [A; **x**], the corresponding row vector is written (**x**; A), and the normal to the planes are generally expressed as row vectors in the reciprocal basis A*. With this notation, any direction [B;**x**] in the bcc basis is transformed into [O;**x**] = ${}_OC_B$[B;**x**] = ${}_BC_O^{-1}$[B;**x**] when the transformation occurs, and any plane of normal (**n**, B*) transforms into a plane which normal in the orthorhombic basis is expressed as (**n**, O*) = (**n**, B*) ${}_BC_O$. The eigenbasis P of the transformation in related to the bcc base by the matrix ${}_PT_B$ [44].

$$ {}_PT_B = \begin{pmatrix} 0 & 0 & \bar{1} \\ \frac{\bar{1}}{\sqrt{2}} & \frac{1}{\sqrt{2}} & 0 \\ \frac{1}{\sqrt{2}} & \frac{1}{\sqrt{2}} & 0 \end{pmatrix} \tag{A.2} $$

If a direction in the hcp basis is given by its four Miller indices [h, k, $-h$ $-k$, l], this direction can be translated into coordinates [O;**x**] = [x_1;x_2;x_3] in the orthorhombic basis via the correspondence matrix ${}_OC_{H^{dir}}$ (consistent with the correspondence given by Srivastava [83]):

$$ \begin{bmatrix} x_1 \\ x_2 \\ x_3 \end{bmatrix} = {}_O\,C_{H^{dir}}. \begin{bmatrix} h \\ k \\ l \end{bmatrix} = \frac{1}{2}\begin{pmatrix} 3 & 0 & 0 \\ 1 & 2 & 0 \\ 0 & 0 & 2 \end{pmatrix} \begin{bmatrix} h \\ k \\ l \end{bmatrix} \tag{A.3} $$

whereas if the indices (h, k, $-$ h $-k$, l) designate a plane, the corresponding plane (**n**, O*) = (n_1, n_2, n_3) in the orthorhombic basis is obtained thanks to the correspondence matrix ${}_HC_{O^{pl}}$ [83]:

$$ \begin{pmatrix} n_1 & n_2 & n_3 \end{pmatrix} = \begin{pmatrix} h & k & l \end{pmatrix}{}_HC_{O^{pl}} = \begin{pmatrix} h & k & l \end{pmatrix} \begin{pmatrix} 1 & 1 & 0 \\ 0 & 2 & 0 \\ 0 & 0 & 1 \end{pmatrix} \tag{A.4} $$

Appendix B. Representation of the surfaces that determine the geometric possibility of forming martensite with an invariant plane strain

Fig. B.10 Fig. B.11 Fig. B.12 Fig. B.13 Fig. B.14.

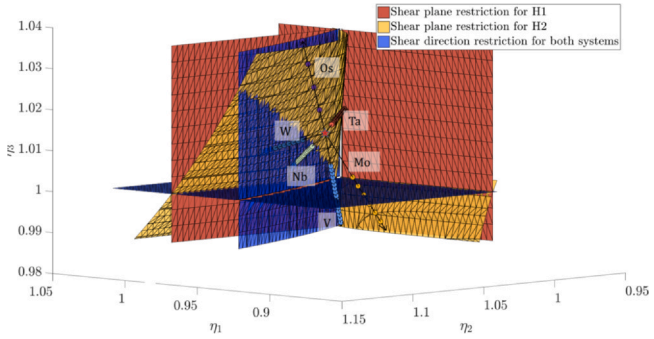

Fig. B.10. Limits for the martensitic transformation to be possible with glide systems H1 and H2, together with eigenvalues for orthorhombic martensitic transformation in some binary Ti-x systems. These binary systems are those for which martensite is known to be orthorhombic above a certain concentration. The arrows represent the extrapolation of the eigenvalues for concentrations for which orthorhombic martensite does not exist (pure Ti and dilute alloys), and each bullet represents an increase of 1 at% in the given alloying element.

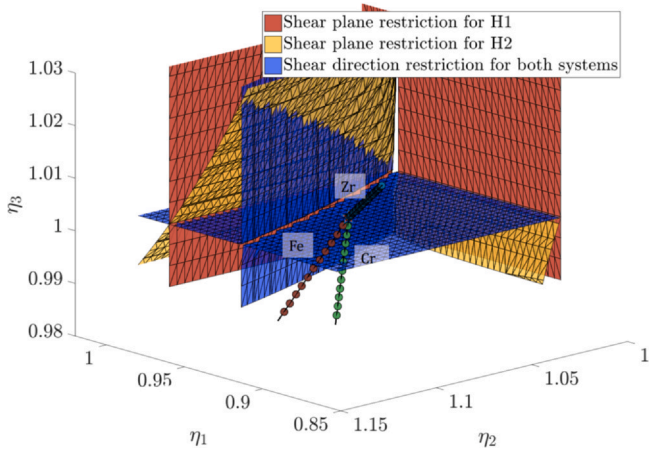

Fig. B.11. Limits for the martensitic transformation to be possible with glide systems H1 and H2, together with eigenvalues for hcp martensitic transformation in some binary Ti-x systems. Starting from pure Ti, each bullet represents an increase of 1 at% in the given alloying element. These binary systems are those which display only hcp martensite and no orthorhombic martensite. Starting from pure Ti, each bullet represents an increase of 1 at% in the given alloying element.

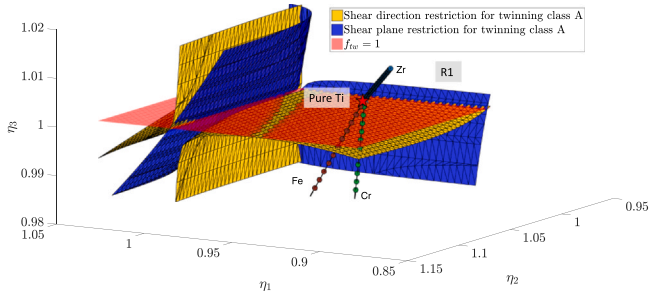

Fig. B.12. Limits for the martensitic transformation to be possible with twinning of type A as LIS, together with eigenvalues for hcp martensitic transformation in some binary Ti-x systems. These binary systems are those which display only hcp martensite and no orthorhombic martensite. Starting from pure Ti, each bullet represents an increase of 1 at% in the given alloying element.

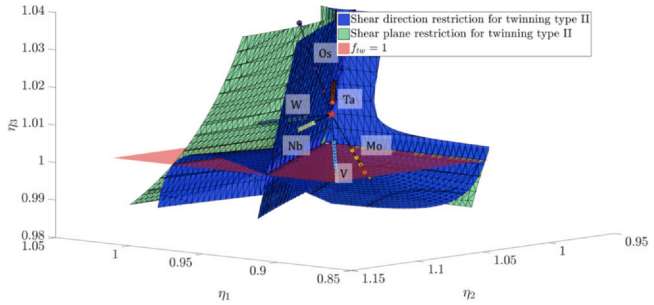

Fig. B.13. Limits for the martensitic transformation to be possible with twinning of type II as LIS, together with eigenvalues for orthorhombic martensitic transformation in some binary Ti-x systems. These binary systems are those for which martensite is known to be orthorhombic above a certain concentration. Starting from pure Ti, each bullet represents an increase of 1 at% in the given alloying element.

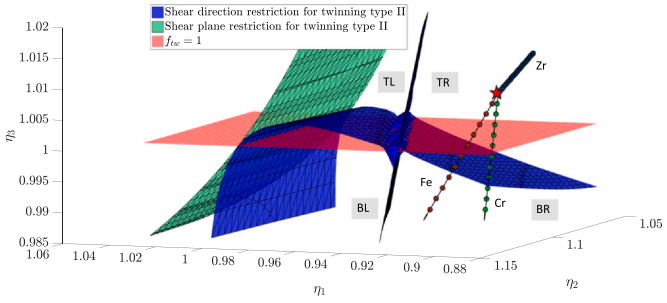

Fig. B.14. Limits for the martensitic transformation to be possible with twinning of type II as LIS, together with eigenvalues for hcp martensitic transformation in some binary Ti-x systems. These binary systems are those which display only hcp martensite and no orthorhombic martensite. Starting from pure Ti, each bullet represents an increase of 1 at% in the given alloying element.

References

[1] T. Grosdidier, M.J. Philippe, Deformation induced martensite and superelasticity in a β-metastable titanium alloy, Mater. Sci. Eng. A 291 (2000) 218–223.

[2] E. Bertrand, P. Castany, T. Gloriant, Investigation of the martensitic transformation and the damping behavior of a superelastic Ti-Ta-Nb alloy, Acta Mater. 61 (2013) 511–518.

[3] P. Castany, T. Gloriant, F. Sun, F. Prima, Design of strain-transformable titanium alloys, Comptes Rendus Phys. 19 (2018) 710–720.

[4] M. Blackburn, Some aspects of phase transformations in titanium alloys, Sci. Technol. Appl. Titan. Sci. Technol. Appl. Titan. Elsevier, 1970, pp. 633–643, https://doi.org/10.1016/B978-0-08-006564-9.50071-3 (https://linkinghub.elsevier.com/retrieve/pii/B9780080065649500713).

[5] T. Duerig, J. Albrecht, D. Richter, P. Fischer, Formation and reversion of stress induced martensite in Ti-10V–2Fe-3Al, Acta Metall. 30 (1982) 2161–2172.

[6] M. Marteleur, F. Sun, T. Gloriant, P. Vermaut, P.J. Jacques, F. Prima, On the design of new β-metastable titanium alloys with improved work hardening rate thanks to simultaneous TRIP and TWIP effects, Scr. Mater. 66 (2012) 749–752.

[7] F. Sun, J. Zhang, C. Brozek, M. Marteleur, M. Veron, E. Rauch, T. Gloriant, P. Vermaut, C. Curfs, P. Jacques, F. Prima, The role of stress induced martensite in ductile metastable beta Ti-alloys showing combined TRIP/TWIP effects, Mater. Today Proc. 2 (2015) S505–S510.

[8] S., Banerjee, P., Mukhopadhyay, Phase Transformations - Examples from Titanium and Zirconium Alloys volume 12 of, Elsevier, 2007. http://www.sciencedirect.com/science/article/pii/S147018040780054X; https://doi.org/10.1016/S1470-1804(07)80054-X.

[9] R., Boyer, G., Welsch, E. W., Collings, Materials Properties Handbook - Titanium Alloys, ASM International, 1994.

[10] E.W. Collings, Applied Superconductivity, Metallurgy, and Physics of Titanium Alloys, Springer US, 1986, https://doi.org/10.1007/978-1-4613-2095-1

[11] L.N. Guseva, L.K. Dolinskaya, Metastable phases in titanium alloys with group VIII elements quenched from the β-region, Russ. Metall. (1974) 155–159.

[12] E. Menon, J. Chakravartty, S. Wadekar, S. Banerjee, Stress induced martensitic transformation in Ti-20V, J. Phys. 43 (1982) C4–321.

[13] S. Hanada, O. Izumi, Correlation of tensile properties, deformation modes, and phase stability in commercial β-phase titanium alloys, Metall. Trans. A 18 (1987) 265–271.

[14] M. Koul, J. Breedis, Phase transformations in beta isomorphous titanium alloys, Acta Metall. 18 (1970) 579–588.

[15] C. Hammond, P. Kelly, The crystallography of titanium alloy martensites, Acta Metall. 17 (1969) 869–882.

[16] S. Banerjee, U.M. Naik, Plastic instability in an omega forming Ti-15% Mo alloy, Acta Mater. 44 (1996) 3667–3677.

[17] A.V. Dobromyslov, V.A. Elkin, Martensitic transformation and metastable β-phase in binary titanium alloys with d-metals of 4-6 periods, Scr. Mater. 44 (2001) 905–910.

[18] D. Qiu, M.X. Zhang, P.M. Kelly, T. Furuhara, Non-classical {3 3 4}β type of twinned α' martensite in a Ti-5.26 wt% Cr alloy, Acta Mater. 67 (2014) 373–382.

[19] P. Duwez, Allotropic transformation in titanium-zirconium alloys, J. Inst. Met. 19 (1952) 525.

[20] P.J.S. Buenconsejo, H.Y. Kim, H. Hosoda, S. Miyazaki, P. John, Shape memory behavior of Ti-Ta and its potential as a high-temperature shape memory alloy, Acta Mater. 57 (2009) 1068–1077.

[21] H.Y. Kim, S. Miyazaki, Martensitic transformation and superelastic properties of Ti-Nb base alloys, Mater. Trans. 56 (2015) 625–634.

[22] A.V. Dobromyslov, V.A. Elkin, The orthorhombic phase in binary titanium-base alloys with d-metals of V-VIII groups, Mater. Sci. Eng. A 438–440 (2006) 324–326.

[23] S. Neelakantan, P.E. Rivera-Díaz-del Castillo, S. van der Zwaag, Prediction of the martensite start temperature for β titanium alloys as a function of composition, Scr. Mater. 60 (2009) 611–614.

[24] J.-Y. Yan, G. Olson, Computational thermodynamics and kinetics of displacive transformations in titanium-based alloys, J. Alloy. Compd. 673 (2016) 441–454.

[25] M. Bignon, E. Bertrand, F. Tancret, P.E. Rivera-Díaz-del Castillo, Modelling martensitic transformation in titanium alloys: the influence of temperature and deformation, Materialia 7 (2019) 100382.

[26] P. Wollants, J.R. Roos, L. Delaey, Thermally- and stress-induced thermoelastic martensitic transformations in the reference frame of equilibrium thermodynamics, Prog. Mater. Sci. 37 (1993) 227–288.

[27] T. Inamura, J.I. Kim, H.Y. Kim, H. Hosoda, K. Wakashima, S. Miyazaki, Composition dependent crystallography of α"-martensite in Ti-Nb-based β-titanium alloy, Philos. Mag. 87 (2007) 3325–3350.

[28] K.A. Bywater, J.W. Christian, Martensitic transformations in titanium-tantalum alloys, Philos. Mag. 25 (1972) 1249–1273.

[29] Y.W. Chai, H.Y. Kim, H. Hosoda, S. Miyazaki, Interfacial defects in Ti-Nb shape memory alloys, Acta Mater. 56 (2008) 3088–3097.

[30] O Ivasishin, N. Kosenko, S Shevchenko, Crystallographic features of α"-martensite in titanium alloys, J. Phys. IV 5 (1995) C8-1017–C8-1022.

[31] B. Sun, X. Meng, Z. Gao, W. Cai, Crystallography study on the internal twinning of Ti-Nb-based shape memory alloys, Cryst. Res. Technol. 53 (2018).

[32] I. Weiss, S.L. Semiatin, Thermomechanical processing of alpha titanium alloys - an overview, Mater. Sci. Eng. A 263 (1999) 243–256.

[33] H. Liu, M. Niinomi, M. Nakai, J. Hieda, K. Cho, Changeable Young's modulus with large elongation-to-failure in β-type titanium alloys for spinal fixation applications, Scr. Mater. 82 (2014) 29–32.

[34] A. Dobromyslov, V. Elkin, The orthorhombic α-ş-phase in binary titanium-base alloys with d-metals of V-VIII groups, Mater. Sci. Eng. A 438–440 (2006) 324–326.

[35] P. Duwez, The martensite transformation temperature in titanium binary alloys. Trans. Am. Soc. Met. 45 (1953) 934–940.

[36] S. Hanada, O. Izumi, Transmission electron microscopic observations of mechanical twinning in metastable beta titanium alloys, Metall. Trans. A 17 (1986) 1409–1420.

[37] F. Sun, J.Y. Zhang, M. Marteleur, T. Gloriant, P. Vermaut, D. Laillé, P. Castany, C. Curfs, P.J. Jacques, F. Prima, Investigation of early stage deformation mechanisms in a metastable β titanium alloy showing combined twinning-induced plasticity and transformation-induced plasticity effects, Acta Mater. 61 (2013) 6406–6417.

[38] H.Y. Kim, Y. Ikehara, J.I. Kim, H. Hosoda, S. Miyazaki, Martensitic transformation, shape memory effect and superelasticity of Ti-Nb binary alloys, Acta Mater. 54 (2006) 2419–2429.

[39] K Jepson, A. Brown, J. Gray, The effect of cooling rate on the beta transformation in Ti-Nb and Ti-Al alloys, Sci. Technol. Appl. Titan. Sci. Technol. Appl. Titan. Elsevier, 1970, pp. 677–690, https://doi.org/10.1016/B978-0-08-006564-9.50074-9 (https://linkinghub.elsevier.com/retrieve/pii/B9780080065649500749).

[40] M. Tahara, N. Okano, T. Inamura, H. Hosoda, Plastic deformation behaviour of single-crystalline martensite of Ti-Nb shape memory alloy, Sci. Rep. 7 (2017) 1–11.

[41] M. Wechsler, D. Lieberman, On the theory of the formation of martensite, Acta Metall. 7 (1959) 793–802.

[42] J.S. Bowles, J.K. Mackenzie, The crystallography of martensite transformations. I the nature of the problem, Acta Metall. 2 (1954) 129–137.

[43] J.K. Mackenzie, J.S. Bowles, The crystallography of martensite transformations II, Acta Metall. 2 (1954) 138–147.

[44] J.S. Bowles, J.K. Mackenzie, The crystallography of martensite transformations III. Face-centred cubic to body-centred tetragonal transformations, Acta Metall. 2 (1954) 224–234.

[45] J.K. Mackenzie, J.S. Bowles, The crystallography of martensite transformations. IV body-centred cubic to orthorhombic transformations, Acta Metall. 5 (1957) 137–149.

[46] H. Bhadeshia, Worked Examples in the Geometry of Crystals, The Institute of Metals, 1987.

[47] J.W., Christian, Crystallography of Martensitic Transformations, in: Theory Transform. Met. Alloy., 2002, 992–1061. https://www.sciencedirect.com/science/article/pii/B9780080440194500271; https://doi.org/10.1016/B978-008044019-4/50027-1.

[48] H.M. Otte, Mechanism of the martensitic transformation in titanium and its alloys, Sci. Technol. Appl. Titan. Pergamon Press Ltd, 1970, pp. 645–657, https://doi.org/10.1016/B978-0-08-006564-9.50072-5

[49] A.G. Crocker, B.A. Bilby, On the theory of martensite crystallography, Acta Metall. 9 (1961) 992–995.

[50] J.-Y. Y. Yan, G.B. Olson, Molar volumes of bcc, hcp, and orthorhombic Ti-base solid solutions at room temperature, Calphad Comput. Coupling Phase Diagr. Thermochem. 52 (2016) 152–158.

[51] G. Aurelio, A. Fernández Guillermet, Assesment of the structural relations between the bcc and omega phases of Ti, Zr, Hf and other transition metals, Z. Met. 31 (2000).

[52] H.Y. Kim, J. Fu, H. Tobe, J.I. Kim, S. Miyazaki, Crystal structure, transformation strain, and superelastic property of Ti-Nb-Zr and Ti-Nb-Ta alloys, Shape Mem. Superelasticity 1 (2015) 107–116.

[53] K. Endoh, M. Tahara, T. Inamura, H. Hosoda, Effect of Sn and Zr addition on the martensitic transformation behavior of Ti-Mo shape memory alloys, J. Alloy. Compd. 695 (2017) 76–82.

[54] G. Aurelio, A. Fernández Guillermet, G.J. Cuello, J. Campo, Metastable phases in the Ti-V system: part I. Neutron diffraction study and assessment of structural properties, Metall. Mater. Trans. A 33 (2002) 1307–1317.

[55] P., Franke, D., Neuschütz, Cr-Ti (chromium-titanium) phase diagram crystal structure, in: Thermodyn. Prop. Inorg. Mater. · Bin. Syst. Part 2 Elem. Bin. Syst. from B - C to Cr - Zr, 2004.

[56] T. Shiraishi, K. Yubuta, T. Shishido, N. Shinozaki, Elastic properties of as-solidified Ti-Zr binary alloys for biomedical applications, Mater. Trans. 57 (2016) 1986–1992.

[57] T. Niendorf, P. Krooß, E. Batyrsina, A. Paulsen, Y. Motemani, A. Ludwig, P. Buenconsejo, J. Frenzel, G. Eggeler, H.J. Maier, Functional and structural fatigue of titanium tantalum high temperature shape memory alloys (HT SMAs), Mater. Sci. Eng. A 620 (2015) 359–366.

[58] N.D. Ross, A.G. Crocker, Type II twinning in martensite crystallography theories, Scr. Metall. 3 (1969) 37–42.

[59] D. Hull, D.J. Bacon, Introduction to Dislocations, Butterworth-Heinemann, 2011.

[60] J.W. Christian, Formal geometry of crystal lattices, Theory Transform. Met. Alloy. (2002), pp. 23–78, https://doi.org/10.1016/b978-008044019-4/50006-4

[61] I. Weiss, S.L. Semiatin, Thermomechanical processing of alpha titanium alloys - an overview, Mater. Sci. Eng. A 263 (1999) 243–256.

[62] J.W. Christian, Accommodation strains in martensite formation, and the use of a dilatation parameter, Acta Metall. 6 (1958) 377–379.

[63] E. Galindo-Nava, On the prediction of martensite formation in metals, Scr. Mater. 138 (2017) 6–11.

[64] H. M., Otte, Transformation in a Titanium - Chromium Alloy, 1954. http://dx.doi.org/10.1038/174506a0.

[65] B. Sun, X.L. Meng, Z.Y. Gao, W. Cai, Martensite structure and mechanical property of Ti-Nb-Ag shape memory alloys for biomedical applications, Vacuum 156 (2018) 181–186.

[66] J. Williams, R. Taggart, D. Polonis, Morphology and substructure of Ti-Cu martensite, Met. Trans. 1 (1970) 2265–2270.

[67] S. Banerjee, R. Krishnan, Martensitic transformation in zirconium-niobium alloys, Acta Metall. 19 (1971) 1317–1326.

[68] X. Ji, I. Gutierrez-Urrutia, S. Emura, T. Liu, T. Hara, X. Min, P. Dehai, K. Tsuchiya, D. Ping, Twinning behavior of orthorhombic-α" martensite in a Ti-7.5Mo alloy, Sci. Technol. Adv. Mater. 20 (2019) 401–411.

[69] J.W., Christian, Deformation twinning, in: Theory Transform. Met. Alloy., 2002, 859–960. https://www.sciencedirect.com/science/article/pii/B9780080440194500258; https://doi.org/10.1016/B978-008044019-4/50025-8.

[70] Z. Nishiyama, M. Oka, H. Nakagawa, $\{10\bar{1}1\}$transformation twins in titanium, Trans. Jpn. Inst. Met. 7 (1966) 174–177.

[71] E. Menon, R. Krishanan, Phase transformations in Ti-V alloys - part 1 martensitic transformations, J. Mater. Sci. 18 (1983) 365–374.

[72] R. Davis, H.M. Flower, D.R.F. West, Martensitic transformations in Ti-Mo alloys, J. Mater. Sci. 14 (1979) 712–722.

[73] K.M. Knowles, D.A. Smith, The crystallography of the martensitic transformation in equiatomic nickel-titanium, Acta Metall. 29 (1981) 101–110.

[74] R.H. Ericksen, R. Taggart, D.H. Polonis, The martensite transformation in Ti-Cr binary alloys, Acta Metall. 17 (1969) 553–564.

[75] S. Weinig, E.S. Machlin, Data for one martensitic transformation in an 11 Pct Mo-Ti alloy, J. Met. (1954) 1280–1281.

[76] Y.C. Liu, Martensitic transformation in binary titanium alloys, Jom 8 (1956) 1036–1040.

[77] P. Gaunt, J.W. Christian, The crystallography of the β-α transformation in zirconium and in two titanium-molybdenum alloys, Acta Metall. 7 (1959) 534–543.

[78] A.J. Williams, R.W. Cahn, C.S. Barrett, The crystallography of the β-α transformation in titanium, Acta Metall. 2 (1954) 117–128.

[79] S.B. Gabriel, J.V. Panaino, I.D. Santos, L.S. Araujo, P.R. Mei, L.H. De Almeida, C.A. Nunes, Characterization of a new beta titanium alloy, Ti-12Mo-3Nb, for biomedical applications, J. Alloy. Compd. 536 (2012) S208–S210.

[80] S. Cai, J.E. Schaffer, Y. Ren, Deformation of a Ti-Nb alloy containing α"-martensite and omega phases, Appl. Phys. Lett. 106 (2015) 131907.

[81] R.M. Wood, Martensitic alpha and omega phases as deformation products in a titanium-15% molybdenum alloy, Acta Metall. 11 (1963) 907–914.

[82] W.G. Burgers, On the process of transition of the cubic-body-centered modification into the hexagonal-close-packed modification of zirconium, Physica 1 (1934) 561–586.

[83] D. Srivastava, S. Banerjee, S. Ranganathan, The crystallography of the bcc to hcp (orthohexagonal) martensitic transformation in dilute Zr-Nb alloys: part I: lattice strain and lattice invariant shear, Trans. Indian Inst. Met. 57 (2004) 205–223.